The role of HYAL2 in LSS-induced glycocalyx impairment and the PKA-mediated decrease in eNOS–Ser-633 phosphorylation and nitric oxide production

Xiangquan Kong[a,b], Liang Chen[a], Peng Ye[a], Zhimei Wang[a], Junjie Zhang[a], Fei Ye[a], and Shaoliang Chen[a,*]

[a]Department of Cardiology, Nanjing First Hospital, Nanjing Medical University, Nanjing 210001, China; [b]Department of Emergency Medicine, Yijishan Hospital, Wannan Medical College, Wuhu 241001, China

ABSTRACT **Hyaluronan (HA) in the endothelial glycocalyx serves as a mechanotransducer for high-shear-stress–stimulated endothelial nitric oxide synthase (eNOS) phosphorylation and nitric oxide (NO) production. Low shear stress (LSS) has been shown to contribute to endothelial inflammation and atherosclerosis by impairing the barrier and mechanotransduction properties of the glycocalyx. Here we focus on the possible role of hyaluronidase 2 (HYAL2) in LSS-induced glycocalyx impairment and the resulting alterations in eNOS phosphorylation and NO production in human umbilical vein endothelial cells (HUVECs). We show that LSS strongly activates HYAL2 to degrade HA in the glycocalyx. The dephosphorylation of eNOS–Ser-633 under LSS was triggered after HA degradation by hyaluronidase and prevented by repairing the glycocalyx with high–molecular weight hyaluronan. Knocking down HYAL2 in HUVECs protected against HA degradation in the glycocalyx by inhibiting the expression and activity of HYAL2 and further blocked the dephosphorylation of eNOS–Ser-633 and the decrease in NO production in response to LSS. The LSS-induced dephosphorylation of PKA was completely abrogated in HYAL2 siRNA–transfected HUVECs. The LSS-induced dephosphorylation of eNOS–Ser-633 was also reversed by the PKA activator 8-Br-cAMP. We thus suggest that LSS inhibits eNOS–Ser-633 phosphorylation and, at least partially, NO production by activating HYAL2 to degrade HA in the glycocalyx.**

Monitoring Editor
Valerie Marie Weaver
University of California, San Francisco

Received: Apr 25, 2016
Revised: Sep 6, 2016
Accepted: Oct 18, 2016

INTRODUCTION

The glycocalyx on the apical surface of endothelial cells forms a protective barrier between the endothelium and flowing blood by promoting the endothelial permeability barrier (Vink and Duling, 2000), binding anticoagulation factors (Rosenberg, 2001), modulating the adhesion of leukocytes to the endothelium (Mulivor and Lipowsky, 2002; Constantinescu *et al.*, 2003), and inhibiting myocardial edema (van den Berg *et al.*, 2003). The glycocalyx consists of acidic oligosaccharides and proteoglycans with glycosaminoglycan side chains (Zeng *et al.*, 2013). Although high shear stress (12–15 dyn/cm^2) has been confirmed to maintain endothelial glycocalyx integrity and resistance to the development of early atherosclerotic lesions (Dai *et al.*, 2004; Gouverneur *et al.*, 2005; van den Berg *et al.*, 2006), low shear stress (LSS; <5 dyn/cm^2) is correlated with the generation and development of endothelial inflammation and atherosclerosis by reducing the size of the glycocalyx, particularly through the degradation of hyaluronan (HA) in the glycocalyx (Florian *et al.*, 2003; Koo *et al.*, 2013). As a common constituent of the endothelial glycocalyx, HA is crucial to endothelial function (Reitsma *et al.*, 2007). In endothelial cells, HA is catabolized by hyaluronidases, such as hyaluronidase 1, hyaluronidase 2 (HYAL2),

This article was published online ahead of print in MBoC in Press (http://www.molbiolcell.org/cgi/doi/10.1091/mbc.E16-04-0241) on October 26, 2016.

*Address correspondence to: Shaoliang Chen (chmengx@126.com).

Abbreviations used: DAPI, 4′,6-diamidino-2-phenylindole; Dio, 3,3′-dioctadecyloxacarbocyanine perchlorate; eNOS, endothelial nitric oxide synthase; FACS, flow cytometry; HA, hyaluronan; HMWHA, high–molecular weight hyaluronan; HUVEC, human umbilical vein endothelial cell; HYAL2, hyaluronidase 2; LMWHA, low–molecular weight hyaluronan; LSS, low shear stress; MFI, mean fluorescence intensity; NO, nitric oxide; qPCR, quantitative real-time PCR.

hyaluronidase 4, and PH-20, under physiological and pathological conditions or by reactive oxygen species under stress conditions (Hrabarova *et al.*, 2011; Østerholt *et al.*, 2012; Dicker *et al.*, 2014). HYAL2 is a glycosylphosphatidylinositol-anchored enzyme attached to the external surface of the plasma membrane and is mainly responsible for clearing extracellular high–molecular weight HA (HMWHA). Thus LSS may reduce the size of the endothelial glycocalyx by increasing HYAL2, which degrades HA on the apical surface of endothelial cells.

Some studies suggested that HA in the glycocalyx can transduce shear stress into endothelial cells and promote nitric oxide (NO) release at high-shear regions (Mochizuki *et al.*, 2003; Thi *et al.*, 2004; Pahakis *et al.*, 2007). Shear stress–induced endothelial NO production is abrogated when endothelial cells are pretreated with hyaluronidase, indicating that HA may contribute to the mechanotransduction of extracellular shear forces to the intracellular compartment. High-shear-stress–stimulated NO production is well known to require the multisite phosphorylation of endothelial nitric oxide synthase (eNOS) by Akt, protein kinase A (PKA), or protein kinase C (Boo *et al.*, 2002a,b; Barauna *et al.*, 2013; Yang and Rizzo, 2013). Although LSS has been proven to impair the endothelial glycocalyx (Gouverneur *et al.*, 2005; van den Berg *et al.*, 2006; Koo *et al.*, 2013), however, little is known regarding changes in eNOS multisite phosphorylation and related mechanisms in response to LSS.

In the present study, we hypothesized that LSS activates HYAL2 to degrade HA within the endothelial glycocalyx in human umbilical vein endothelial cells (HUVECs). Then we examined how LSS reduced NO production after HA degradation in the glycocalyx by LSS-activated HYAL2. Our results confirmed that LSS strongly activates HYAL2, which leads to HA injury within the endothelial glycocalyx and the dephosphorylation of eNOS at Ser-633. Knocking down HYAL2 inhibited HA degradation in the glycocalyx, resulting in the restoration of eNOS–Ser-633 phosphorylation and the partial recovery of NO production under LSS. Similar results were also observed with exogenous HMWHA. The deactivation of eNOS–Ser-633 by LSS in HA-deficient HUVECs was due to the dephosphorylation of PKA. These findings provide important new insights and suggest that HYAL2 inhibition can protect the endothelial glycocalyx and restore NO production to some degree under LSS.

RESULTS

HA levels in HUVECs are down-regulated by LSS

To test the hypothesis that LSS reduces HA in the glycocalyx, we measured HA by immunostaining HUVECs exposed to LSS for 5, 15, 30, and 60 min; cells without LSS treatment served as a control. Figure 1 shows that the down-regulation of HA was apparent not only in the glycocalyx but also in the cytoplasm as early as 15 min after LSS onset and persisted for at least 60 min. Our result agrees with those of previous experiments (van den Berg *et al.*, 2006; Potter and Damiano, 2008; Koo *et al.*, 2013).

LSS-stimulated HA impairment occurs via HYAL2

Numerous studies have led to a tentative model for HA degradation in which HYAL2 cleaves extracellular matrix HA into small fragments that are then endocytosed and degraded in lysosomes by hyaluronidase 1 (Stern, 2003, 2004). To explore whether HA in the glycocalyx was degraded by activated HYAL2 in response to LSS, we first examined cell membrane HYAL2 protein expression after the cells were subjected to LSS for 0, 5, 15, 30, and 60 min. As shown in Figure 2A, surface HYAL2 protein expression was markedly elevated after 15 min of LSS exposure and reached a maximum by 30 min.

Next HUVECs were transiently transfected with HYAL2-siRNA using Lipofectamine RNAiMAX. After the HUVECs were fully differentiated, quantitative real-time PCR (qPCR) and Western blot experiments showed that HYAL2 mRNA and membrane protein expression decreased to ~45.0 and 41.6%, respectively. HYAL2-silenced cells were then exposed to LSS for 30 min. HYAL2-siRNA significantly suppressed the LSS-induced increase in HYAL2 mRNA (Figure 2B) and protein expression (Figure 2C). Optimum pH for HYAL2 activity is 6.8 (range, 6.0–7.0). HYAL2 activity was also up-regulated in HUVECs in response to LSS treatment for 30 min. HYAL2-siRNA significantly inhibited LSS-induced HYAL2 activation (Figure 2D).

Because endothelial HA expression is affected by several factors, such as hyaluronidases, HA synthases, CD44, superoxide, and peroxynitrite (Monzon *et al.*, 2010; Hrabarova *et al.*, 2011; Dicker *et al.*, 2014), we further investigated whether HA degradation in the glycocalyx under LSS was mediated by HYAL2. HA expression was assessed by immunostaining. To locate HA in the glycocalyx, we labeled the cell membrane with 3,3′-dioctadecyloxacarbocyanine perchlorate (Dio). HA in the glycocalyx layer was present in the cell membrane and extracellular matrix and was quantified according to the mean fluorescence intensity (MFI) and thickness. Figure 2E indicates that HYAL2 silencing partially reversed the LSS-stimulated reduction in the MFI of HA in the glycocalyx. To determine the precise change in the thickness of the glycocalyx, we compared *XY*- to *XZ*- or *YZ*-slices in a three-dimensional reconstruction of a single image. The maximum thickness of HA in the glycocalyx layer was measured as 1.47 μm. LSS led to thinning of the glycocalyx via HYAL2 activation (Figure 2E). The results show that HYAL2 small interfering RNA (siRNA) inhibited LSS-induced HA degradation in the glycocalyx but not in the cytoplasm.

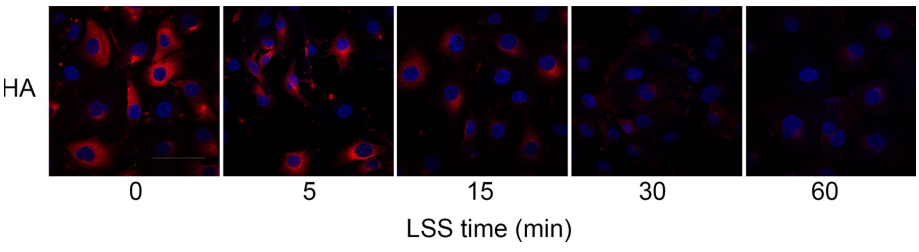

FIGURE 1: LSS decreases HA expression in HUVECs. Confluent monolayers of HUVECs were exposed to LSS for 0, 5, 15, 30, and 60 min. HA was visualized with a monoclonal sheep anti-hyaluronan antibody followed by an Alexa Fluor 647–conjugated secondary antibody (red), and nuclei were visualized with DAPI (blue). Bar, 10 μm. HA expression exhibited a remarkable time-dependent decrease starting after 15 min in response to LSS in three independent experiments.

HYAL2 is involved in the LSS-mediated dephosphorylation of eNOS at Ser-633

To explore the effect of LSS on the multisite phosphorylation of eNOS, we first tested the phosphorylation of eNOS at Ser-1177, Thr-495, and Ser-633 in HUVECs exposed to LSS of 2 dyn/cm^2 for 5, 15, 30, and 60 min. Figure 3A shows that eNOS–Ser-1177 was activated in a time-independent manner starting at 5 min of LSS exposure, whereas eNOS–Thr-495 phosphorylation showed a time-dependent increase starting at 15 min of LSS exposure. A 15-min LSS exposure was required to observe a marked decrease in eNOS–Ser-633 phosphorylation, which

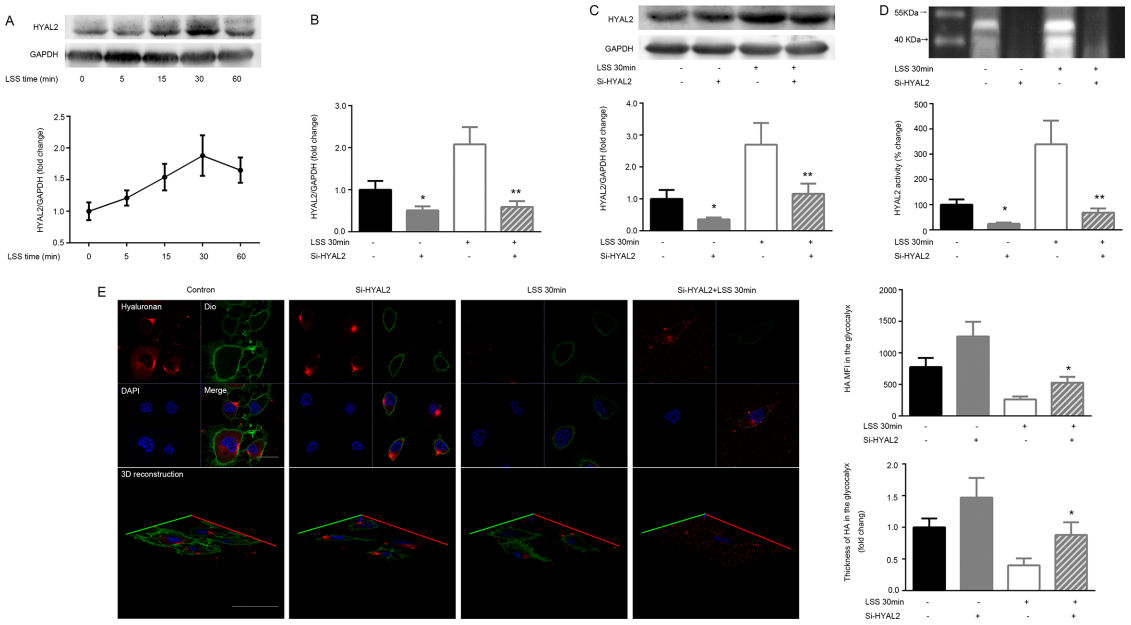

FIGURE 2: HA in the glycocalyx is degraded by LSS-activated HYAL2. Confluent monolayers of HUVECs were exposed to LSS for 0, 5, 15, 30, and 60 min. Western blotting was used to analyze HYAL2 protein levels on the cell membrane. HYAL2-siRNA (Si-HYAL2) was stably transfected into HUVECs, followed by a 30-min LSS exposure. HYAL2 mRNA levels were evaluated via qPCR. Numerical data were standardized to GAPDH. The results are averages from three independent experiments (mean ± SEM). (A) HYAL2 protein expression on the cell membrane was significantly elevated as early as 15 min after shear onset and reached a maximum by 30 min. (B) Cells without LSS or HYAL2-siRNA were used as controls. HYAL2 mRNA expression was reduced to ~45.0% in HUVECs transfected with HYAL2-siRNA; *$p < 0.01$ vs. control, **$p < 0.01$ vs. LSS 30 min. (C) HYAL2 protein levels on the cell membrane were down-regulated to ~41.6% and were not significantly restored by LSS in HUVECs transfected with HYAL2-siRNA; *$p < 0.05$ vs. control, **$p < 0.05$ vs. LSS 30 min. (D) An HA zymogram was used to explore HYAL2 activity. Band intensities were analyzed using Quantity One software, and HYAL2 activity was expressed as percentage change in band intensity per square millimeter compared with control. Each bar represents the mean ± SEM of three separate experiments. HYAL2 activity was attenuated in HUVECs transfected with HYAL2-siRNA. LSS greatly increased HYAL2 activity within 30 min in control HUVECs but did not stimulate HYAL2 activity in HYAL2-siRNA–transfected HUVECs; *$p < 0.01$ vs. control, **$p < 0.01$ vs. LSS 30 min. (E) Stably transfected cells were exposed to LSS for 30 min. Samples were analyzed via indirect immunofluorescence and confocal microscopy. HA was visualized with an anti-HA antibody followed by an Alexa Fluor 647–conjugated secondary antibody (red), and nuclei were visualized with DAPI (blue). The cell membrane was identified with Dio (green). Bar, 10 μm. HA MFI and thickness in the glycocalyx layer were measured to reveal changes in the glycocalyx under LSS. LSS-induced down-regulation of HA MFI in the glycocalyx was significantly inhibited by HYAL2 siRNA. Similar alterations were observed in HA thickness. Each bar represents mean ± SEM of three or four separate experiments; *$p < 0.05$ vs. LSS 30 min.

persisted for at least 60 min. In HYAL2-silenced HUVECs, only the dephosphorylation of eNOS–Ser-633 was reversed in response to LSS (Figure 3B). HYAL2 did not participate in the altered eNOS phosphorylation at Ser-1177 and Thr-495 induced by LSS.

The dephosphorylation of eNOS–Ser-633 depends on HA degradation in the glycocalyx by activated HYAL2 under LSS.

To examine how LSS-activated HYAL2 attenuated the phosphorylation of eNOS–Ser-633, we exposed HUVECs to LSS in the presence of 25 μg/ml HMWHA, which binds specifically to the cell membrane to repair glycocalyx injured by LSS. Low–molecular weight hyaluronan (LMWHA) (5 μg/l) was used to exclude the effect of LMWHA produced by activated HYAL2 on glycocalyx thickness and the phosphorylation of eNOS–Ser-633. Immunofluorescence staining suggested that exogenous HMWHA effectively restored HA levels in the endothelial glycocalyx to 82 ± 15.5% of control levels within 30 min of LSS exposure. Figure 4A shows that the dephosphorylation of eNOS–Ser-633 in response to LSS was significantly blocked by HMWHA. Despite having been described as a type of "danger signal" in many studies, LMWHA had no effect on HA thickness in the glycocalyx layer or on the level of eNOS–Ser-633 phosphorylation. To further confirm the role of diminished glycocalyx protection in contributing to lower eNOS–Ser-633 phosphorylation levels, we incubated HUVECs with 1.5 IU/ml hyaluronidase for 3 h before a 5-min LSS exposure. Figure 4B demonstrates that eNOS–Ser-633 was dephosphorylated by LSS within 5 min in HA-degraded endothelial cells.

LSS-induced dephosphorylation of eNOS–Ser-633 is regulated by PKA signaling linked to glycocalyx injury

To clarify whether the LSS-mediated reduction in eNOS–Ser-633 phosphorylation was mediated by PKA in glycocalyx-deficient HUVECs, we first investigated the effect of LSS on the phosphorylation of PKA. PKA phosphorylation underwent a time-dependent decrease starting at 15 min of LSS exposure (Figure 5A). Next we verified that LSS did not stimulate the dephosphorylation of PKA in HYAL2 siRNA–transfected cells (Figure 5B). Repairing the LSS-injured glycocalyx with HMWHA also blocked PKA inactivity (Figure 5C). Furthermore, the PKA activator 8-Br-cAMP (1 mM) was used to treat the cells before initiation of LSS for 30 min. Figure 6D shows that 8-Br-cAMP significantly induced PKA activity compared

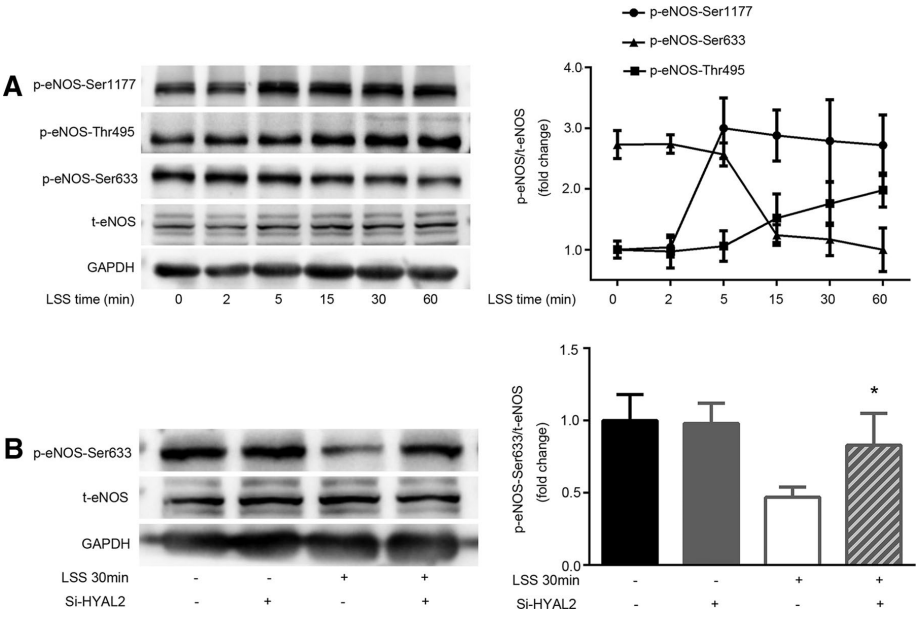

FIGURE 3: HYAL2 participates in the LSS-mediated dephosphorylation of eNOS–Ser-633. Western blotting of eNOS using antibodies specific for total proteins, eNOS phosphorylated at Ser1-177 (P-eNOS–Ser-1177), Thr-495 (P-eNOS–Th-r495), and Ser-633 (p-eNOS–Ser-633) and total eNOS (t-eNOS). Numerical data averaged from at least three independent experiments after normalization to t-eNOS. Statistically significant increases in eNOS–Ser-1177 and –Thr-495 phosphorylation were detected after 5 and 15 min of LSS exposure, respectively. eNOS–Ser-633 phosphorylation decreased markedly after 15 min of LSS exposure. However, only the alteration in eNOS–Ser-633 phosphorylation due to LSS was abolished in HYAL2 siRNA–transfected HUVECs. Intensity of each band was quantified as described in *Materials and Methods*. Line graphs represent mean ± SEM of three or four separate experiments; *$p < 0.05$ vs. LSS 30 min.

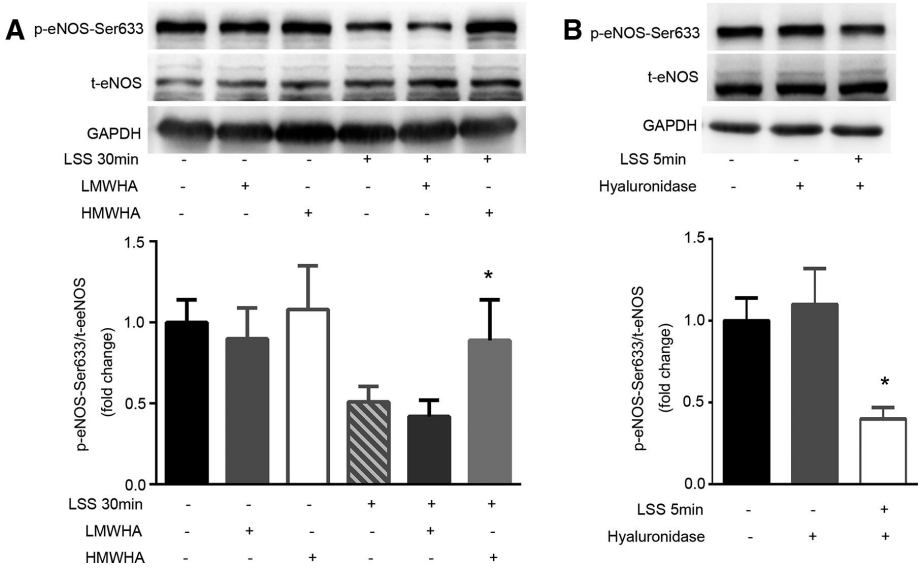

FIGURE 4: Glycocalyx injury by activated HYAL2 plays a key role in the dephosphorylation of eNOS at Ser-633 under LSS. (A) Confluent monolayers of HUVECs were exposed to LSS in the presence of 25 µg/ml HMWHA or 5 µg/l LMWHA for 30 min. Total protein extracts from HUVECs were separated by SDS–PAGE and analyzed by Western blotting using anti-eNOS, anti–eNOS-Ser-633, or anti-GAPDH antibodies. t-eNOS expression was used for normalization. Each bar represents mean ± SEM of three or four separate experiments. HMWHA inhibited the LSS-induced dephosphorylation of eNOS–Ser-633; *$p < 0.05$ vs. LSS 30 min. (B) HUVECs were pretreated with vehicle (0.9% sodium chloride) or 1.5 IU/ml hyaluronidase for 3 h before exposure to LSS for 5 min. Western blotting of eNOS, eNOS–Ser-633, and GAPDH using specific antibodies. Western blotting showed eNOS–Ser-633 was dephosphorylated by LSS within 5 min in HA-degraded HUVECs. Numerical data were normalized to t-eNOS. Each bar represents mean ± SEM of three or four separate experiments; *$p < 0.01$ vs. LSS 5 min.

with that of the control group. Treating cells with 8-Br-cAMP for 30 min significantly prevented LSS-trigged eNOS–Ser-633 dephosphorylation. However, 8-Br-cAMP did not affect LSS-induced HYAL2 activity and HA impairment.

Protecting the glycocalyx partly reverses the LSS-mediated decrease in NO production via the PKA/eNOS–Ser-633 pathway

To clarify the effect of LSS-induced HA degradation on NO production in HUVECs, we exposed HYAL2 siRNA–transfected cells to LSS for 30 min. HYAL2 siRNA–transfected cells and control cells were treated with LSS for 30 min in the presence or absence of 25 µg/ml HMWHA or 1 mM 8-Br-cAMP. NO production was measured via flow cytometry (FACS) using the NO-specific fluorescent dye 3-amino, 4-aminomethyl-2,7′-difluorescein diacetate (DAF-FM DA). As shown in Figure 7, HYAL2 knockdown markedly blocked the negative effect of LSS on NO production. Restoring the glycocalyx with exogenous HMWHA or activating PKA with 8-Br-cAMP also reversed NO release.

DISCUSSION

High shear stress has been shown to thicken the endothelial glycocalyx by increasing endothelial HA synthase 2–mediated HA synthesis and stimulating the incorporation of HA into the endothelial cell glycocalyx (Gouverneur *et al.*, 2006; Maroski *et al.*, 2011). However, many studies suggest that LSS promotes atherosclerosis by thinning the glycocalyx layer, especially by degrading HA in the glycocalyx (van den Berg *et al.*, 2006; Maroski *et al.*, 2011; Koo *et al.*, 2013). Although LSS is well known to induce glycocalyx injury, little is known about the mechanisms and consequences of glycocalyx injury due to LSS. In the present work, we explored LSS-induced HA degradation in the glycocalyx via the hyaluronidase pathway in HUVECs and its possible role in regulating eNOS phosphorylation and NO production.

We primarily found that exposure to LSS increased HYAL2 activity and accelerated HA catabolism in HUVECs. The cells displayed a 3.4-fold increase in HYAL2 activity after exposure to LSS for 30 min. Exposure to LSS for >15 min down-regulated HA expression not only in the glycocalyx but also in the cytoplasm. Silencing HYAL2 inhibited LSS-induced HA degradation in the glycocalyx but not in the cytoplasm. These results demonstrate that activated HYAL2 is responsible for glycocalyx impairment under LSS. We do not know how LSS activates HYAL2. Some studies showed that reactive oxygen species (ROI) increase HYAL2 expression and activity

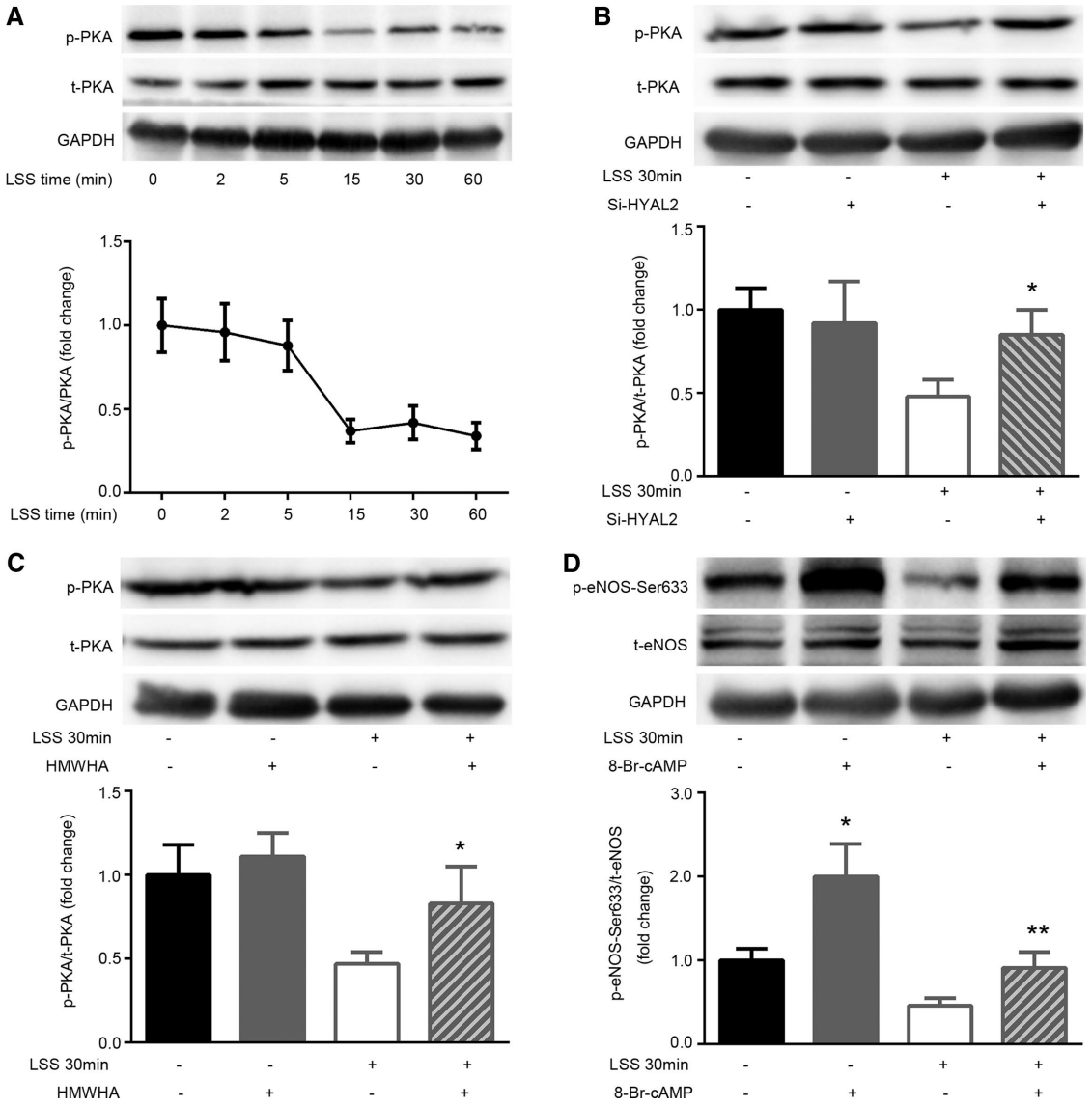

FIGURE 5: Glycocalyx injury contributes to PKA-regulated eNOS–Ser-633 dephosphorylation under LSS. (A) Confluent monolayers of HUVECs were exposed to LSS for 0, 5, 15, 30, and 60 min. Western blotting of total PKA (t-PKA), phosphorylated PKA (p-PKA), and GAPDH using specific antibodies. Numerical data were normalized to t-PKA. PKA phosphorylation significantly decreased after 15 min of LSS exposure. The line graphs represent mean ± SEM of three or four separate experiments. (B) HYAL2-siRNA was stably transfected into HUVECs, followed by exposure to LSS for 30 min. Western blotting of t-PKA, p-PKA, and GAPDH using specific antibodies. Numerical data were normalized to t-PKA. HYAL2 siRNA prevented the LSS-induced deactivation of PKA. Each bar represents the mean ± SEM of three or four separate experiments; *$p < 0.05$ vs. LSS 30 min. (C) HUVECs were exposed to LSS in the presence of 25 μg/ml HMWHA for 30 min. Western blotting of eNOS, eNOS–Ser-633, and GAPDH using specific antibodies. The LSS-induced dephosphorylation of PKA was reversed by HMWHA; *$p < 0.05$ vs. LSS 30 min. (D) HUVECs were pretreated with vehicle (dimethyl sulfoxide) or the PKA activator 8-Br-cAMP (1 mmol/l) for 30 min before exposure to LSS for 30 min. Western blotting of eNOS, eNOS–Ser-633, and GAPDH using specific antibodies. eNOS–Ser-633 phosphorylation was markedly increased by 8-Br-cAMP. The attenuation of eNOS–Ser-633 phosphorylation in response to LSS was abrogated by 1 mmol/l 8-Br-cAMP. Each bar represents the mean ± SEM of three or four separate experiments; *$p < 0.01$ vs. control, **$p < 0.05$ vs. LSS 30 min.

in normal human bronchial epithelial cells via p38 mitogen-activated protein kinase signaling (Monzon *et al.*, 2010). Our laboratory previously reported increased ROS levels in HUVECs in response to LSS (Wang *et al.*, 2014). Therefore HA impairment in the glycocalyx due to LSS-induced HYAL2 is perhaps mediated by ROS. However, HA can also be fragmented directly by the ROS generated by many types of cells under stress conditions (Soltes *et al.*, 2006). These results suggest that ROS probably participate in LSS-stimulated HYAL2 activity and HA degradation. HYAL2 is a well-known acid-active enzyme. Perhaps LSS activates Na^+-H^+ exchanger activity, which creates an acidic extracellular matrix environment and leads to HYAL2-mediated HA catabolism.

We further explored how LSS promoted altered eNOS phosphorylation and NO production in glycocalyx-deficient HUVECs. First, we found that LSS stimulated changes in eNOS multisite phosphorylation and NO release. Then we confirmed that activated HYAL2 contributes to the eNOS-Ser-633–mediated decrease in NO production in HYAL2 siRNA–transfected HUVECs in response to

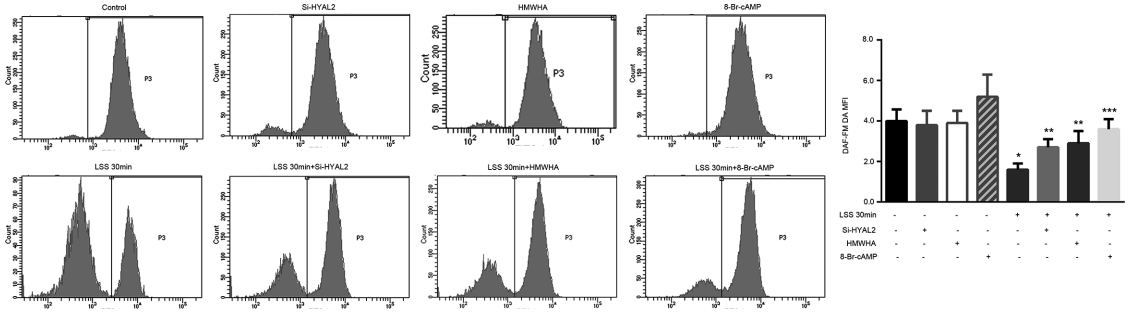

FIGURE 6: LSS-induced reduction in NO production is partly reversed by restoring the glycocalyx or activating PKA. HYAL2-siRNA was stably transfected into HUVECs, followed by LSS exposure for 30 min. Other cells were exposed to LSS in the presence of 25 μg/ml HMWHA or 1 mmol/l 8-Br-cAMP. HUVEC NO was stained using the NO-specific fluorescent dye DAF-FM DA. The MFI of DAF-FM DA was determined via FACS. LSS significantly inhibited NO synthesis. The decrease in NO production due to LSS was partly blocked in HUVECs transfected with HYAL2-siRNA. Both HMWHA and 8-Br-cAMP reversed NO production under LSS. Each bar represents the mean ± SEM of three or four separate experiments; *$p < 0.05$ vs. control; **$p < 0.05$ vs. LSS 30 min; ***$p < 0.01$ vs. LSS 30 min.

LSS. Finally, the finding that repairing the glycocalyx with HMWHA reversed LSS-induced endothelial injury confirmed that HYAL2 was not directly involved in this adverse effect and instead degraded the glycocalyx and left the endothelial cells without glycocalyx protection against LSS, leading to the down-regulation of eNOS–Ser-633 phosphorylation and NO production. This result demonstrated that HA in the glycocalyx protects endothelial cells from LSS injury. Previous studies suggested that hyaluronidase-mediated HA impairment in the glycocalyx layer significantly decreased flow-induced endothelial NO production (Mochizuki *et al.*, 2003; Pahakis *et al.*, 2007). These studies only indicated that HA plays a specific role in the mechanotransduction of endothelial shear stress. Another characteristic of the glycocalyx is to confer barrier properties to endothelial cells by forming the first protective "sieve" (Constantinescu *et al.*, 2003; VanTeeffelen *et al.*, 2007). This hypothesis was confirmed in our present study.

Moreover, immunofluorescence confirmed that exogenous HMWHA significantly increased the fluorescence intensity of cell surface HA and increased glycocalyx thickness before LSS disruption. However, LMWHA treatment did not have a similar effect (Figure 7). These findings suggested that HMWHA binds effectively to the cell surface and are consistent with a previous report (Fieber *et al.*, 2004).

The mechanisms underlying shear stress–mediated eNOS phosphorylation and NO production are complicated. Work by Boo *et al.* (2002b) supports the idea that high-shear-stress–dependent phosphorylation of eNOS–Ser-635, which is a major PKA site in bovine eNOS and is homologous to eNOS–Ser-633 in human cells, is regulated in a PKA-dependent manner in bovine aortic endothelial cells. Our results show that eNOS–Ser-633 phosphorylation and NO levels were significantly decreased after the dephosphorylation of PKA by LSS in HUVECs, which was prevented by PKA activation using 8-Br-cAMP. Thus we suggest that PKA is an upstream mediator of eNOS phosphorylation at Ser-633 in response to LSS. From this evidence, we might also infer that the effect of shear stress on eNOS–Ser-633 and PKA phosphorylation depends on the magnitude of the shear stress. A few studies showed that eNOS and PKA colocalize in cell junctions (Heijnen *et al.*, 2004). This colocalization provides favorable conditions for PKA to phosphorylate eNOS. However, HA degradation in the glycocalyx layer destroys the cell junctions and increases endothelial permeability (van den Berg *et al.*, 2003). Therefore we hypothesize that LSS inhibits the colocalization of PKA and eNOS in cell-to-cell contact sites by weakening the endothelial glycocalyx to prevent PKA from activating eNOS. Cheng *et al.* (2005) reported that shear stress affected the intracellular distribution of eNOS, which might have an effect on interactions between PKA and eNOS.

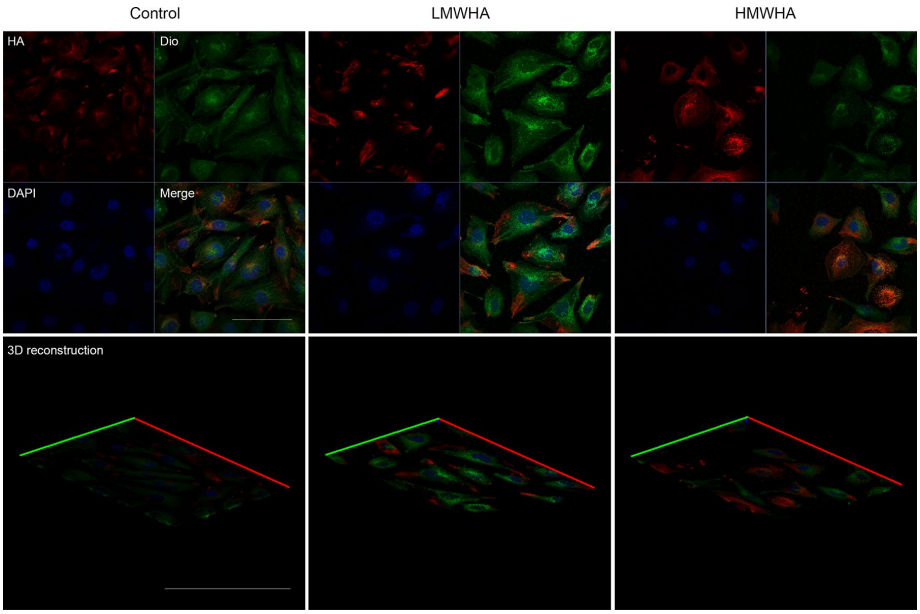

FIGURE 7: Exogenous HMWHA can bind specifically to the cell membrane. HUVECs were treated with 25 μg/ml HMWHA or 5 μg/l LMWHA for 3 h. HA was visualized with an anti-HA antibody followed by an Alexa Fluor 647–conjugated secondary antibody (red), and nuclei were visualized with DAPI (blue). The cell membrane was identified with Dio (green). Bar, 10 μm. HMWHA significantly increased not only the fluorescence intensity of cell surface HA but also glycocalyx thickness in three independent experiments. However, LMWHA had no effect on HA MFI and glycocalyx thickness.

Overall our findings indicate that the LSS-induced degradation of HA in the glycocalyx of HUVECs depends on HYAL2 activity. The LSS-induced dephosphorylation of eNOS–Ser-633 mediated by PKA is attributed to the lack of barrier properties but not the reduced mechanotransduction ability of the glycocalyx. Our conclusions not only demonstrate the mechanism of glycocalyx injury under LSS but also confirm that LSS-induced endothelial impairment is partly based on the loss of the glycocalyx barrier. Furthermore, HYAL2 is revealed as a possible target for preventing LSS-induced glycocalyx injury.

MATERIALS AND METHODS

Cell culture

HUVECs were obtained from the American Type Culture Collection. Cells were maintained in DMEM (Life Technologies, Waltham, MA) supplemented with 10% fetal bovine serum (FBS; Life Technologies), 100 μg/ml streptomycin, and 100 U/ml penicillin at 37°C under 5% CO_2.

LSS studies

The parallel flow chamber designed by the Shanghai Medical Instrument School was previously described (Zhang *et al.*, 2014). Briefly, cells were grown to confluence on a coverslip and placed in the chamber, which was established by sandwiching a silicon gasket between two stainless steel plates with a coverslip sink in the base plate. A heart pump simulator was connected to the chamber, and different levels of shear stress were obtained by modulating the proportion of fluid volume passing through the flow chamber. The shear stress in our experiments was 2 dyn/cm^2.

Western blotting

HUVECs were lysed, and total protein was extracted on ice with RIPA buffer containing a protease inhibitor (Sigma-Aldrich, St. Louis, MO) and a phosphatase inhibitor. Membrane proteins were extracted using the CelLytic MEM Protein Extraction Kit (Sigma-Aldrich) according to the manufacturer's protocol. Homogenates were centrifuged at 12,000 × *g* for 20 min at 4°C. The protein concentration was determined using a bicinchoninic acid protein assay according to manufacturer's instructions (KeyGen Biotech, Nanjing, China). Equal amounts of protein were resolved via 10% SDS–PAGE and electrophoretically transferred to polyvinylidene difluoride membranes.

Membranes were blocked for 2 h with 5% FBS in Tris-buffered saline/Tween-20 (TBST) or phosphate-buffered saline/Tween-20 (PBST) buffer at room temperature and then incubated overnight with 1:1000 dilutions of primary antibodies at 4°C. The following primary antibodies were used: monoclonal rabbit antibodies against phospho–eNOS-Thr-495/Ser-1177, total eNOS, phospho-PKA, and total PKA from Cell Signaling Technology (Beverly, MA); a monoclonal mouse antibody against phospho-eNOS (Ser-633) from BD Biosciences; and a monoclonal rabbit antibody against HYAL2 from Abcam (Cambridge, United Kingdom). Hyaluronic acid sodium salt from *Streptococcus equi* (HMWHA, 500–750 kDa; LMWHA, 8–15 kDa) was obtained from Sigma-Aldrich. The membranes were washed three times with TBST or PBST and then incubated with alkaline phosphatase–conjugated secondary antibodies (1 h at room temperature); bands were visualized using chemiluminescence. The intensities of the immunoreactive bands in Western blots were analyzed with ImageJ software (National Institutes of Health, Bethesda, MD).

HYAL2 silencing

HUVECs were transfected at ~50% confluence. The cells were starved in DMEM containing 5% FBS for 2 h. Specific HYAL2 Stealth siRNA, which was used at 100 nM siRNA per 1.5 × 10^5 cells, was designed and synthesized by Invitrogen (Carlsbad, CA; sense, 5′-AAUAUUGGGUGGCCCAGGACACAUU-3′; antisense, 5′-AAUGUGUCCUGGGCCACCCAAUAUU-3′) and transfected using Lipofectamine RNAiMAX. Noncoding Stealth RNA was used as control. Transfection efficiency and degree of HYAL2 silencing were evaluated using qPCR and Western blotting 48 h after transfection.

Enzyme treatment using hyaluronidase

We used hyaluronidase from *Streptomyces hyalurolyticus* (Sigma-Aldrich). This enzyme cleaves HA at the β-D-GalNAc-(1→4)-β-D-GlcA bond and specifically targets the HA component of the endothelial glycocalyx. PBS was used to wash the sample gently three times before the cells were incubated in DMEM supplemented with 10% FBS and 1.5 IU/ml hyaluronidase for 3 h at 37°C. At the end of the incubation, HUVECs were immediately subjected to LSS or stained. The removal of HA was verified with an enzyme-linked immunosorbent assay kit from R&D as previously described (Pahakis *et al.*, 2007).

Immunofluorescence staining

HUVECs were fixed briefly with 4% paraformaldehyde for 20 min and washed with phosphate buffer at room temperature. The cells were incubated overnight with a sheep monoclonal antibody against HA (1:100; Abcam) at 4°C. Then HA was visualized using the appropriate Alexa Fluor 647–conjugated donkey anti-sheep immunoglobulin G (H + L) secondary antibody, (Life Technologies) for 2 h. The cell membrane was visualized with 10 μM Dio (Beyotime, Shanghai, China) for 20 min at room temperature. Nuclei were stained with 1 μM 4′,6-diamidino-2-phenylindole (DAPI; Invitrogen) for 10 min.

HA zymography

Hyaluronidase activity was assayed via HA zymography as previously described (Monzon *et al.*, 2010). Briefly, the samples were electrophoresed in 10% polyacrylamide gels containing 0.17 mg/ml HA from *Streptococcus zooepidemicus* (Sigma-Aldrich) followed by a 2-h incubation in 0.3% Triton X-100 at room temperature. The gels were subsequently incubated overnight in 0.15 M NaCl containing 0.1 M sodium formate, pH 3.7, at 37°C and then stained with 0.5% Alcian blue containing 3% acetic acid for 16 h. HYAL2 activity was visualized as clear bands on the blue background. Band intensities were recorded with a GelDoc XRS system (Bio-Rad) and analyzed using Quantity One software (Bio-Rad). The results were expressed as percentage change in intensity (INT) per square millimeter of surface.

RNA extraction and qPCR

Total RNA was extracted from cells using TRIzol reagent (Invitrogen) according to the manufacturer's instructions. To generate cDNA, the following primer pairs were used: HYAL2 (accession number NM_003773): forward primer, 5′-GGCCCCACCGTTACATTGG-3′, and reverse primer, 5′-ATTCTGGTTCACAAAACCCTCAT-3′ (207 base pairs); and glyceraldehyde-3-phosphate dehydrogenase (GAPDH; accession number NM_002046): forward primer, 5′-CCTGACCTGCCGTCTAGAAA-3′, and reverse primer, 5′-TACTCCTTGGAGGCCATGTG-3′ (276 base pairs). All RNA sequences were designed and produced by Invitrogen. Total RNA was reverse transcribed into cDNA using a PrimeScript first-strand cDNA Synthesis Kit (Takara, Dalian, China), and amplification was performed using SYBR Premix Ex Taq (Takara). HYAL2 mRNA expression was measured via qPCR, starting with 600 s at 95°C and followed by 40 cycles of denaturation (95°C for 15 s), annealing (60°C, 60 s), and elongation (72°C, 75 s). Relative quantification was calculated by normalizing the $2^{-\Delta\Delta Ct}$ values to those of GAPDH.

Flow cytometry analysis

Intracellular NO was analyzed using the NO-specific fluorescent dye DAF-FM DA (Life Technologies; Garczorz *et al*., 2015). Briefly, cells were loaded with 5 μM DAF-FM DA at 37°C for 30 min in the dark. Cells were then rinsed three times with PBS and kept in the dark. We assessed NO levels by examining the fluorescence intensity of the DAF-FM DA–stained cells. The X-mean values of DAF-FM DA from FACS were used to assess cellular NO levels.

Statistical analysis

Statistical analysis was performed using one-way analysis of variance followed by the least significant difference (L) test. $p < 0.05$ based on at least three or more independent experiments was considered statistically significant.

ACKNOWLEDGMENTS

This study was supported by the National Natural Science Foundation of China (Grant 91439118). We gratefully acknowledge Yu-Lin Gu (Nature-Think Company, Shanghai, China) for technical support with the mechanics of the parallel flow chamber.

REFERENCES

Barauna VG, Mantuan PR, Magalhaes FC, Campos LC, Krieger JE (2013). AT1 receptor blocker potentiates shear-stress induced nitric oxide production via modulation of eNOS phosphorylation of residues Thr (495) and Ser (1177). Biochem Biophys Res Commun 441, 713–719.

Boo YC, Hwang J, Sykes M, Michell BJ, Kemp BE, Lum H, Jo H (2002b). Shear stress stimulates phosphorylation of eNOS at Ser (635) by a protein kinase A-dependent mechanism. Am J Physiol Heart Circ Physiol 283, 1819–1828.

Boo YC, Sorescu G, Boyd N, Shiojima I, Walsh K, Du J, Jo H (2002a). Shear stress stimulates phosphorylation of endothelial nitric-oxide synthase at Ser1179 by Akt-independent mechanisms: role of protein kinase A. J Biol Chem 277, 3388–3396.

Cheng C, van Haperen R, de Waard M, van Damme LC, Tempel D, Hanemaaijer L, van Cappellen GW, Bos J, Slager CJ, Duncker DJ, *et al*. (2005). Shear stress affects the intracellular distribution of eNOS: direct demonstration by a novel in vivo technique. Blood 106, 3691–3698.

Constantinescu AA, Vink H, Spaan JA (2003). Endothelial cell glycocalyx modulates immobilization of leukocytes at the endothelial surface. Arterioscler Thromb Vasc Biol 23, 1541–1547.

Dai G, Kaazempur-Mofrad MR, Natarajan S, Zhang Y, Vaughn S, Blackman BR, Kamm RD, Garcia-Cardena G Jr, Gimbrone MA (2004). Distinct endothelial phenotypes evoked by arterial waveforms derived from atherosclerosis-susceptible and -resistant regions of human vasculature. Proc Natl Acad Sci USA 101, 14871–14876.

Dicker KT, Gurski LA, Pradhan-Bhatt S, Witt RL, Farach-Carson MC, Jia X (2014). Hyaluronan: a simple polysaccharide with diverse biological functions. Acta Biomater 10, 1558–1570.

Fieber C, Baumann P, Vallon R, Termeer C, Simon JC, Hofmann M, Angel P, Herrlich P, Sleeman JP (2004). Hyaluronan-oligosaccharide-induced transcription of metalloproteases. J Cell Sci 15, 359–367.

Florian JA, Kosky JR, Ainslie K, Pang Z, Dull RO, Tarbell JM (2003). Heparan sulfate proteoglycan is a mechanosensor on endothelial cells. Circ Res 93, 136–142.

Garczorz W, Francuz T, Siemianowicz K, Kosowska A, Klych A, Aghdam MR, Jagoda K (2015). Effects of incretin agonists on endothelial nitric oxide synthase expression and nitric oxide synthesis in human coronary artery endothelial cells exposed to TNFα and glycated albumin. Pharmacol Rep 67, 69–77.

Gouverneur M, Berg B, Nieuwdorp M, Stroes E, Vink H (2006). Vasculoprotective properties of the endothelial glycocalyx: effects of fluid shear stress. J Intern Med 259, 393–400.

Gouverneur M, Spaan JA, Pannekoek H, Fontijn RD, Vink H (2005). Fluid shear stress stimulates incorporation of hyaluronan into endothelial cell glycocalyx. Am J Physiol Heart Circ Physiol 290, 452–458.

Heijnen HF, Waaijenborg S, Crapo JD, Bowler RP, Akkerman JW, Slot JW (2004). Colocalization of eNOS and the catalytic subunit of PKA in endothelial cell junctions: a clue for regulated NO production. J Histochem Cytochem 52, 1277–1285.

Hrabarova E, Juranek I, Soltes L (2011). Pro-oxidative effect of peroxynitrite regarding biological systems: a special focus on high-molar-mass hyaluronan degradation. Gen Physiol Biophys 30, 223–238.

Koo A, Dewey CF Jr, Garcia-Cardena G (2013). Hemodynamic shear stress characteristic of atherosclerosis-resistant regions promotes glycocalyx formation in cultured endothelial cells. Am J Physiol Cell Physiol 304, 137–146.

Maroski J, Vorderwulbecke BJ, Fiedorowicz K, Da Silva-Azevedo L, Siegel G, Marki A, Pries AR, Zakrzewicz A (2011). Shear stress increases endothelial hyaluronan synthase 2 and hyaluronan synthesis especially in regard to an atheroprotective flow profile. Exp Physiol 96, 977–986.

Mochizuki S, Vink H, Hiramatsu O, Kajita T, Shigeto F, Spaan JA, Kajiya F (2003). Role of hyaluronic acid glycosaminoglycans in shear-induced endothelium-derived nitric oxide release. Am J Physiol Heart Circ Physiol 285, 722–726.

Monzon ME, Fregien N, Schmid N, Falcon NS, Campos M, Casalino-Matsuda SM, Forteza RM (2010). Reactive oxygen species and hyaluronidase 2 regulate airway epithelial hyaluronan fragmentation. J Biol Chem 285, 26126–26134.

Mulivor AW, Lipowsky HH (2002). Role of glycocalyx in leukocyte-endothelial cell adhesion. Am J Physiol Heart Circ Physiol 283, 1282–1291.

Østerholt HC, Dannevig I, Wyckoff MH, Liao J, Akgul Y, Ramgopal M, Mija DS, Cheong N, Longoria C, Mahendroo M, *et al*. (2012). Antioxidant protects against increases in low molecular weight hyaluronan and inflammation in asphyxiated newborn pigs resuscitated with 100% oxygen. PLoS One 7, 38839.

Pahakis MY, Kosky JR, Dull RO, Tarbell JM (2007). The role of endothelial glycocalyx components in mechanotransduction of fluid shear stress. Biochem Biophys Res Commun 355, 228–233.

Potter DR, Damiano ER (2008). The hydrodynamically relevant endothelial cell glycocalyx observed in vivo is absent in vitro. Circ Res 102, 770–776.

Reitsma S, Slaaf DW, Vink H, van Zandvoort MA, Egbrink MG Oude (2007). The endothelial glycocalyx: composition, functions, and visualization. Pflugers Arch 454, 345–359.

Rosenberg RD (2001). Redesigning heparin. N Engl J Med 344, 673–675.

Soltes L, Mendichi R, Kogan G, Schiller J, Stankovska M, Arnhold J (2006). Degradative action of reactive oxygen species on hyaluronan. Biomacromolecules 7, 659–668.

Stern R (2003). Devising a pathway for hyaluronan catabolism: are we there yet? Glycobiology 13, 105–115.

Stern R (2004). Hyaluronan catabolism: a new metabolic pathway. Eur J Cell Biol 83, 317–325.

Thi MM, Tarbell JM, Weinbaum S, Spray DC (2004). The role of the glycocalyx in reorganization of the actin cytoskeleton under fluid shear stress: a "bumper-car" model. Proc Natl Acad Sci USA 101, 16483–16488.

van den Berg BM, Spaan JA, Rolf TM, Vink H (2006). Atherogenic region and diet diminish glycocalyx dimension and increase intima-to-media ratios at murine carotid artery bifurcation. Am J Physiol Heart Circ Physiol 290, 915–920.

van den Berg BM, Vink H, Spaan JA (2003). The endothelial glycocalyx protects against myocardial edema. Circ Res 92, 592–594.

VanTeeffelen JW, Brands J, Jansen C, Spaan JA, Vink H (2007). Heparin impairs glycocalyx barrier properties and attenuates shear dependent vasodilation in mice. Hypertension 50, 261–267.

Vink H, Duling BR (2000). Capillary endothelial surface layer selectively reduces plasma solute distribution volume. Am J Physiol Heart Circ Physiol 278, 285–289.

Wang Z, Zhang J, Li B, Gao X, Liu Y, Mao W, Chen SL (2014). Resveratrol ameliorates low shear stressinduced oxidative stress by suppressing ERK/eNOSThr495 in endothelial cells. Mol Med Rep 10, 1964–1972.

Yang B, Rizzo V (2013). Shear stress activates eNOS at the endothelial apical surface through β1 containing integrins and caveolae. Cell Mol Bioeng 6, 346–354.

Zeng Y, Waters M, Andrews M, Honarmandi P, Ebong EE, Rizzo V, Tarbell JM (2013). Fluid shear stress induces the clustering of heparan sulfate via mobility of glypican-1 in lipid rafts. Am J Physiol Heart Circ Physiol 305, 811–820.

Zhang J, Wang Z, Zhang J, Zuo G, Li B, Mao W, Chen S (2014). Rapamycin attenuates endothelial apoptosis induced by low shear stress via mTOR and sestrin1 related redox regulation. Mediators Inflamm 2014, 769608.